



Fatigue Resistance of Oxygen Cut Steel

Fatigue life is strongly influenced by oxygen cut surface roughness, and fractography indicates that resolidified metal deposits at the torch edge of a cut may often be the site of fatigue crack initiation

BY R. PLECKI, R. YESKE, C. ALTSTETTER AND F. V. LAWRENCE, JR.

ABSTRACT. Oxygen cut surfaces of controlled roughnesses were prepared. Fatigue specimens of high strength, low alloy (ASTM A572) and high strength, quenched-and-tempered (ASTM A514) grades of steel were prepared with four controlled surface roughnesses. Load-controlled fatigue tests were performed using a zero-to-tension stress cycle. The surface roughness was quantified by the RMS deviation from flatness, and the sub-surface microstructures were characterized metallographically and by microhardness measurements.

Fatigue life was found to be strongly influenced by roughness, and to differ by as much as an order of magnitude between rough and smooth surfaces at the lowest stress levels. Fractography indicated that resolidified metal deposits at the torch edge of the cut were often the site of fatigue crack initiation.

The effect of oxygen cutting on fatigue life could be qualitatively understood on the basis of the stress concentration resulting from an array of surface notches.

Introduction

The oxygen cutting of thick steel sections is an economical alternative to other cutting and shaping methods, particularly if little further machining

or grinding of the cut edge is required. In fatigue applications, the surface and sub-surface regions exert a strong influence on behavior; thus, it is necessary to assess the impact of oxygen cutting in these regions. In addition to the modification of surface properties due to chemical changes, microstructural changes and changes in the state of residual stress, changes in geometrical features such as roughness, gouges, drag lines, melted beads and cracks may be introduced by oxygen cutting.

The effect of oxygen cutting on fatigue life has been previously studied in mild steel having a ferrite-pearlite microstructure, and results of different investigators vary widely.¹⁻⁴ Processing variables have been found to significantly modify the steel hardness and microstructure. However, these variables have not always been systematically controlled, and the state of the metal has been quite variable.

R. PLECKI is Research Assistant, R. YESKE is Assistant Professor, C. ALTSTETTER is Professor, Department of Metallurgy and Mining, and F. V. LAWRENCE, JR., is Associate Professor, Departments of Civil Engineering and Metallurgy and Mining, University of Illinois at Urbana-Champaign, Urbana, Illinois.

For example, Koenigsberger^{1,2} and co-workers have reported both the presence and the absence of significant surface hardening, sub-surface softening, and through-thickness softening (32 mm) for different suppliers of oxygen cut specimens. The Netherlands group³ has reported surface hardnesses ranging from 245 VHN to well over double that value as a result of changes in preheating procedure, nozzle type, gas type and pressures, and cutting speed. Even Goldberg,⁴ who defined surface quality and carefully quantified the surface roughness, found wide variability in hardness changes.

Despite these changes in the material, the generally held view is that excessive surface roughness decreases the fatigue life, and surface roughening is the most important result of oxygen cutting.

The principal objective of the present work was to extend the current knowledge of fatigue behavior of oxygen cut surfaces to a higher stress regime. Thus high strength, low alloy (ASTM A572) and quenched-and-tempered steels (ASTM A514) were investigated at short lifetimes. Surface roughness was varied in a controlled manner. The microstructure and hardness profiles were determined for each roughness and steel type. The fatigue

Table 1—Mechanical Properties

| Material | Yield strength S_y , ksi | Ultimate strength S_u , ksi | Strain at fracture e_f , % |
|----------------------------------|----------------------------|-------------------------------|------------------------------|
| A572 ^(a) | 55 | 79 | 23 |
| A514 ^(a) | 108.3 | 119.0 | 15.2 |
| A514 (normalized) ^(b) | 52.0 | 77.0 | — |

^(a)Supplied by manufacturer.

^(b)Overall specimen length 12 in., 1 in. gage length, 0.5 in. diameter reduced section.

results could be rationalized by the stress concentration effects of a periodic array of notches.

Experimental Procedure

Two structural steels were obtained as 1 in. (25 mm) thick plate. One was comparable to ASTM A572 grade 42 0.22% max. carbon, 42 ksi (290 MPa) minimum yield strength, and the second was a quenched-and-tempered steel which conformed to ASTM A514 grade C (0.2% max. carbon, 0.005% max. boron, 100 ksi (609 MPa) minimum yield strength).

The tensile properties of these materials are given in Table 1. The plates were cut into 12 in. (305 mm) squares and milled to the cross-section shown in Fig. 1. Specimens of a varying roughness were oxygen cut from these blanks by moving them beneath a cutting torch which was oscillated at different amplitudes and frequencies.

The cutting parameters were as follows: #1 tip, propylene gas at 5 psig (34 KPa), preheat oxygen at 7 psig (48 KPa), cutting oxygen at 50 psig (345 KPa), average cutting speed 9 ipm (3.8 mm/s) and torch tip to metal separation of 1/4 in. (6 mm). After cutting, one side of the specimen was milled parallel to the opposite oxygen cut surface to give a 3/4 in. square test

section. All specimens were wire brushed by hand before testing. Specimens were mounted in an MTS machine using self-aligning grips and were fatigue tested using a zero-to-tension stress cycle ($R = 0$) under load control at 5–15 Hz.

The contour of the oxygen cut surface of each specimen was measured using an LVDT profilometer with a tungsten carbide stylus inclined 30 degrees from the surface normal. Profile traces were recorded at the midpoint and at the melted (upper) edge. The RMS amplitude of deviation from flatness was used to characterize the notch-peak distribution.

Figure 2 shows traces and photographs of the four roughness levels used in this study: 0.001, 0.002, 0.007, and 0.011 in. (25, 50, 180, and 280 μm). Triplicate fatigue tests were run at each of two stress levels and four roughness levels for each steel. Specimens of the quenched-and-tempered steel were also normalized after oxygen cutting and then tested. A limited number of tests were also performed on machined specimens.

Following fatigue testing, selected specimens were sectioned and mounted for optical metallography and SEM fractography. Microhardness profiles normal to the oxygen cut surface were determined using a

Knoop indenter and 100 gram (gm) load.

Results

Metallography and Microhardness

Oxygen cutting produces a variety of microstructures and several kinds of hardness profile. At many points along the surface of either steel, there was a decarburized layer, particularly where oxide droplets had solidified on the surface. These nodules of resolidified metal were invariably decarburized and were light etched with 3% nital—Fig. 3. Microhardness measurements verified that these regions were much softer than the adjacent metal. Further evidence of decarburization was the absence of pearlite in these regions after specimens were normalized (in vacuum).

Below the decarburized zone was a relatively hard zone in both steels. In A572 steel, the microconstituent was acicular, and its character changed from coarse Widmanstatten ferrite just under the surface to the appearance of bainite and then martensite. In the A514 steel, just under the decarburized zone was a dark etching, fine grained, martensitic zone extending to about 0.04 in. (1.0 mm) below the surface. Beyond this zone was the intercritical heat-affected zone (HAZ), consisting of coarse ferrite grains with some very fine pearlite colonies at the grain boundaries.

In one specimen of A514, there was a second zone of coarse ferrite and pearlite at 0.14–0.18 in. (3.6 to 4.6 mm). Other specimens of A514 showed only a single such zone. The intercritical HAZ in the A572 steel extended from about 0.06 to 0.10 in. (1.5 to 2.5 mm) below the surface. In both steels, the HAZ extended as much as 0.2 in. (5 mm) below the surface.

Figures 4 and 5 are microhardness traverses across the HAZ of a sample of each type of steel. There was a more distinct tendency for the A514 to show plateaus of hardness which could be correlated to the different microstructures. In A572 under the martensitic zone, there was a general decrease in hardness which followed the observed modifications of pearlite in a ferrite matrix.

Fatigue Test Results

The results of the fatigue tests for the two steels are plotted in Figs. 6 and 7. The RMS roughness was measured for each fatigue specimen and the points in Figs. 6 and 7 are correspondingly identified. A number of specimens broke in the grips, thereby decreasing the number of data points somewhat. For this reason, scatter

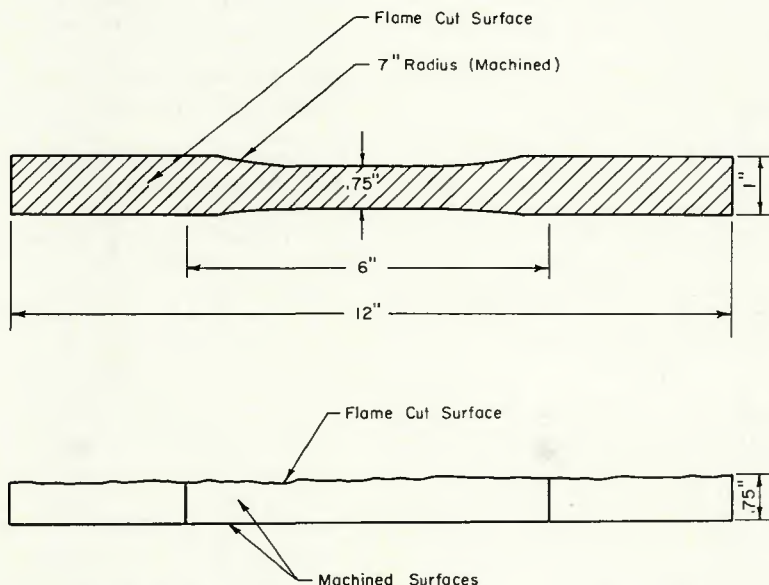


Fig. 1—Specimen geometry

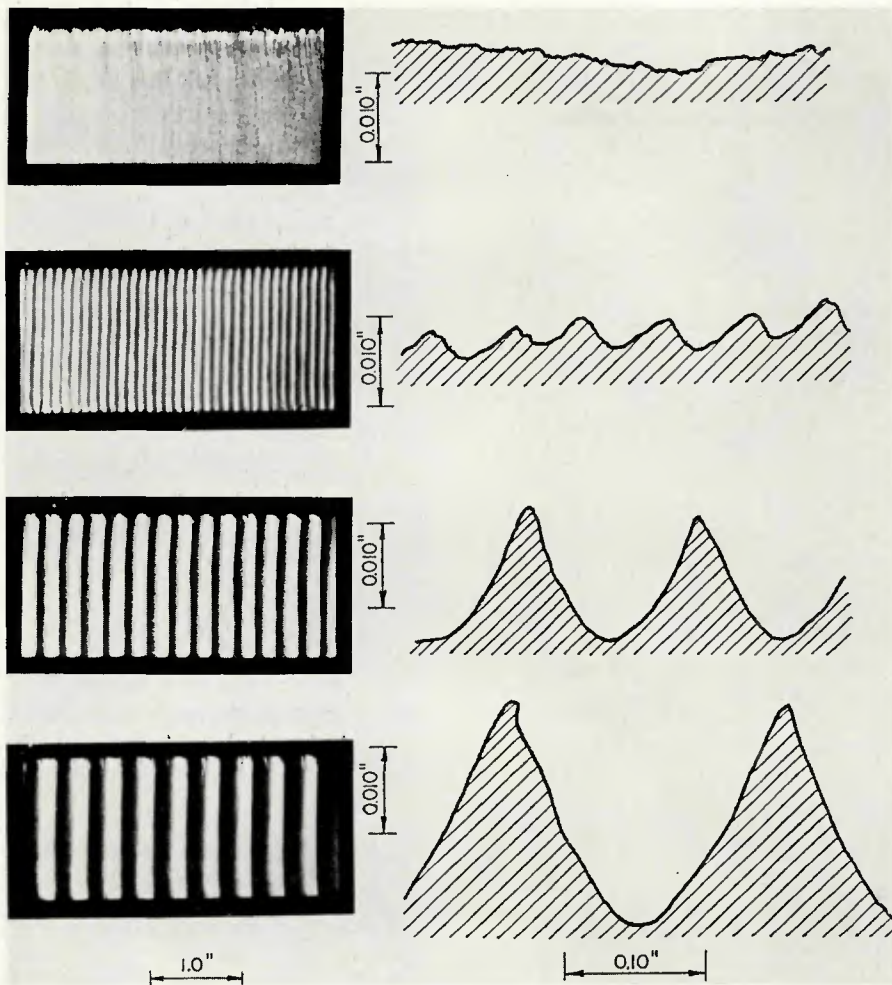


Fig. 2—Profilometer traces and macrographs of the four oxygen-cut surfaces studied

bands have not been assigned in a rigorous way. The lines in Figs. 6 and 7 are least-squares fits for the roughest and smoothest specimens.

Comparison of the results for the smoothest flame cut surface (Figs. 6 and 7) shows that the higher strength A514 steel has a higher fatigue resistance than the A572 at 10^5 cycles. At 10^6 cycles the fatigue strengths of the A514 and A572 steels are for all purposes identical. The A514 steel exhibited a greater sensitivity to rough oxygen cut surfaces in that for a given fatigue life the allowable stress level was degraded more severely by a rough oxygen cut in A514 than in A572 steel; this is partly due to the greater slope of the S-N plot for A514.

Fractography

The fatigue failures almost always initiated at the upper edge, closest to the torch. At this edge there was generally more resolidified metal. At this point also, there is a less regular topography with somewhat greater RMS roughness—Fig. 8.

Figure 9 shows a crack in A514 steel initiating at the edge of a decarburized droplet on the surface. When viewed

in the SEM at up to $\times 1000$, the oxygen cut surfaces were smoothly contoured in some places and dendritic in others. The fatigue cracks were often seen to

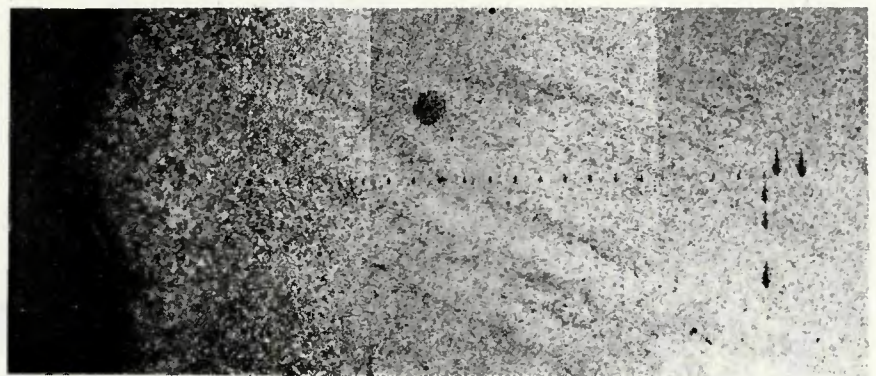


Fig. 4—Oxygen cut surface of A514 steel specimen: top—microstructural modifications; bottom—microhardness variation

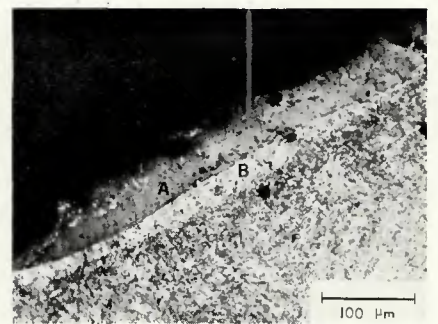
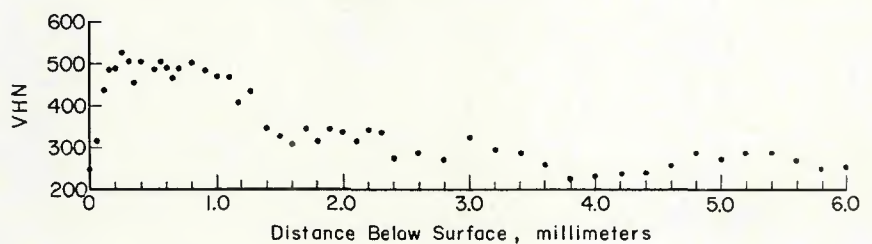


Fig. 3—Oxide layer (A) at oxygen-cut surface of A514 steel specimen adjacent to underlying decarburized zone (B)

follow the interdendritic spaces and the boundary between smooth and dendritic areas. The fracture surfaces themselves showed largely transgranular cracks with some crack branching.

Discussion

Stress Concentration at Notches

The simplest treatment of the effect of oxygen cutting on fatigue is to disregard all but the geometrical features of the oxygen cut surface. A model for the effect of oxygen cutting was developed by assuming that the surface contour can be approximated as a series of notches. Assuming elastic behavior, the theoretical stress concentration factor, K_t , at a single notch tip is defined simply as the ratio of the maximum longitudinal stress at the tip, σ_t , to the average, remote stress, S .

$$K_t = \sigma_t / S \quad (1)$$

For an elliptical surface notch of depth, t , and root radius, r (see Fig. 10)

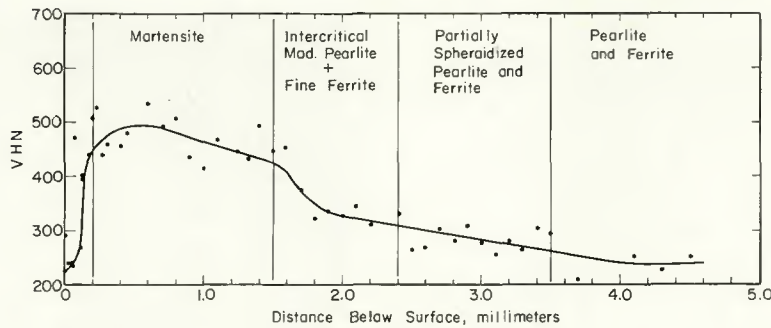


Fig. 5—Microhardness variation in A572 oxygen-cut steel

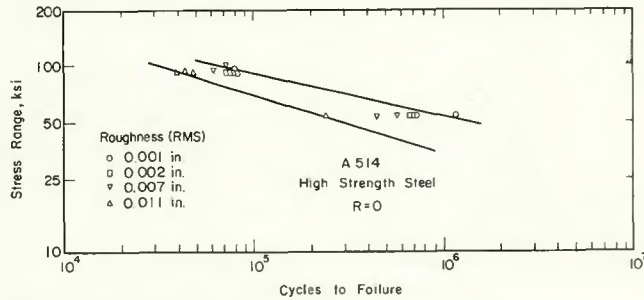


Fig. 6—S-N diagram for A514 steel specimens

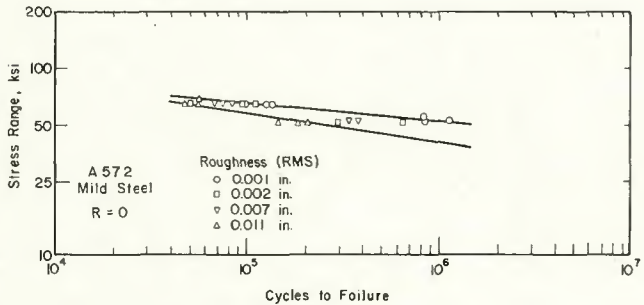


Fig. 7—S-N diagram for A572 steel specimens

the elastic stress concentration factor for a single notch is approximately

$$K_t \approx 1 + 2 \left(\frac{t}{r}\right)^{1/2} \quad (2)$$

For the case of a semicircular notch, this expression reduces to $K_t = 3$. At higher values of notch acuity, t/r , the theoretical elastic stress concentration may reach quite high values, as shown in Fig. 11.

A periodic, infinite array of notches is far less detrimental than a single

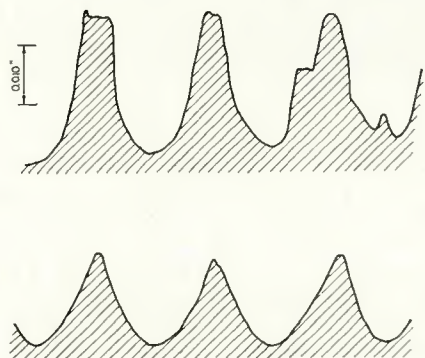


Fig. 8—Topography of oxygen-cut surface: top—at torch edge; bottom—at midsection

notch. The value of K_t for such an array depends not only upon the notch acuity, but also on the notch spacing,

b. In the limit of large spacing, K_t for the array approaches that for a single notch. For the case of semicircular notches, Fig. 12 illustrates that (for a finite array) the stress concentration is intermediate between that of a single notch and an infinite array.⁵ Furthermore, K_t decreases with the number of notches and is greater for the end notch than for the center notch.

For the more realistic case of elliptical notches, it was assumed that the percent reduction in K_t for an array will be roughly the same as that found for semicircular notches.

Effect of Notches on Fatigue

The elastic stress concentration factor is appropriate only under completely elastic conditions. However, there is always some small amount of notch root plasticity, especially in fatigue loading. Therefore, the K_t values given by eqs. 1 and 2 and graphically shown in Figs. 11 and 12 must be modified for fatigue. The fatigue notch factor, K_f , is defined as the ratio of fatigue strengths of unnotched to notched specimens at long lives and

$$K_f = \frac{S(\text{smooth})}{S(\text{notched})} \quad (3)$$

is usually less than K_t because of plasticity effects. Peterson⁶ has found that these effects can be empirically accounted for by a material property, a , where

$$K_f \approx 1 + \frac{K_t - 1}{1 + a/r} \quad (4)$$

For steels the value of (a) can be related to the ultimate tensile strength S_u ,

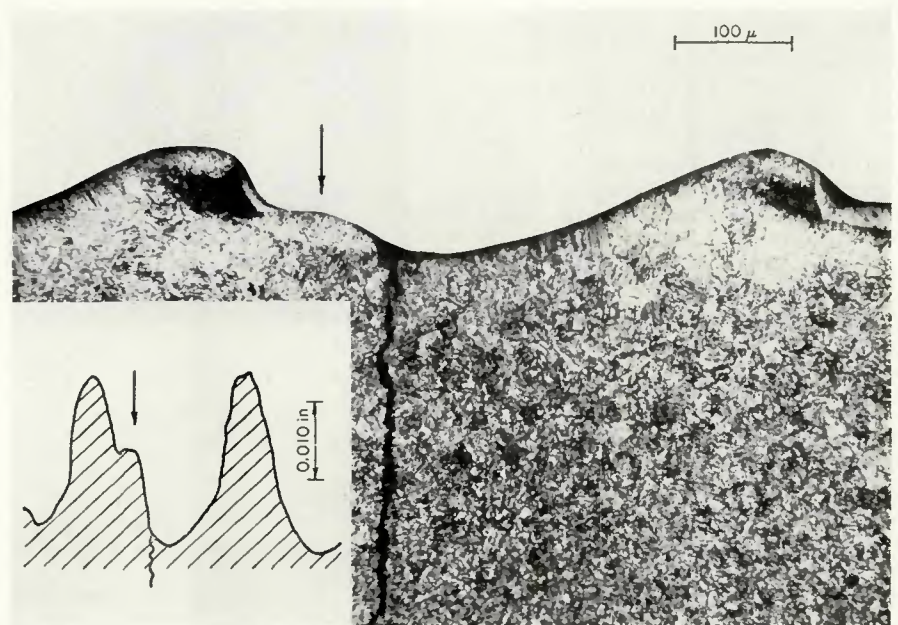


Fig. 9—Fatigue crack originating at decarburized, resolidified metal

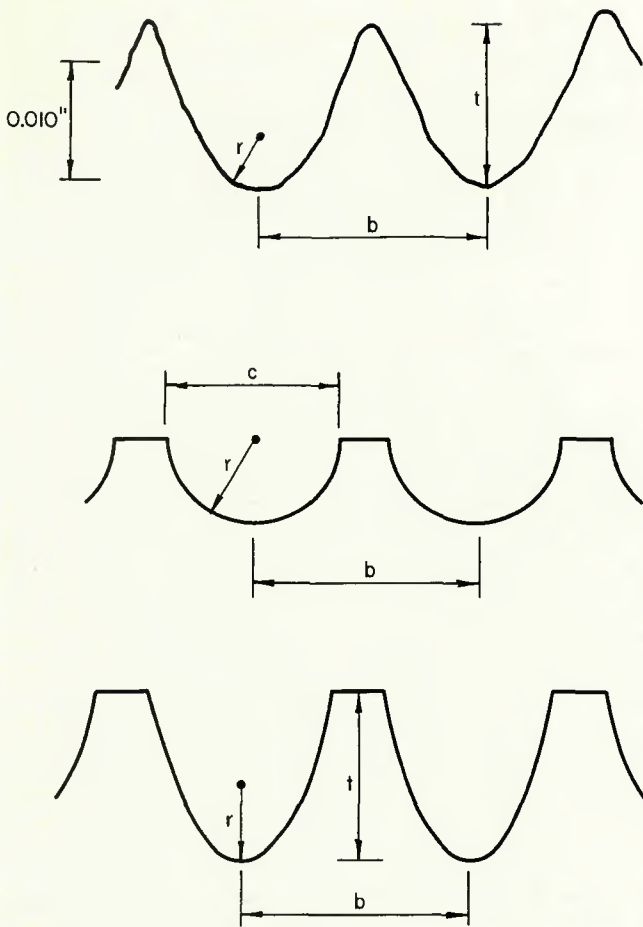


Fig. 10—Actual (top) and idealized oxygen-cut surface topographies

$$a = .001 \left(\frac{300}{S_u} \right)^{1.8} \quad (5)$$

where S_u is given in ksi, and (a) is in inches.

Fatigue Resistance of Oxygen Cut Surface

As seen in Figs. 6 and 7 the fatigue resistance of specimens with oxygen cut surfaces decreased with increasing roughness, particularly at longer lives, where the state of stress at the notch tips approaches elastic conditions. This is in agreement with previously stated relationships.

In order to place this trend on a more quantitative basis, the geometrical parameters, r , t , b and c were estimated for the different roughness levels tested. K_t values were then calculated for both semicircular and elliptical notches. Using the base metal S_u values for each steel, the factor K_t was calculated for both semicircular and elliptical notch arrays for the roughest surfaces tested.

The calculated values are shown in Table 2 and compared with experimentally determined values. The latter were estimated using eq. (3). To minimize the effect of microstructural alteration due to oxygen cutting, the

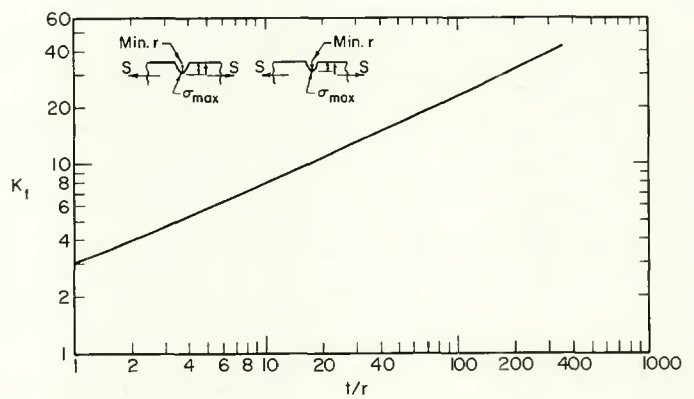


Fig. 11—Elastic stress concentration factor for single surface notch⁵

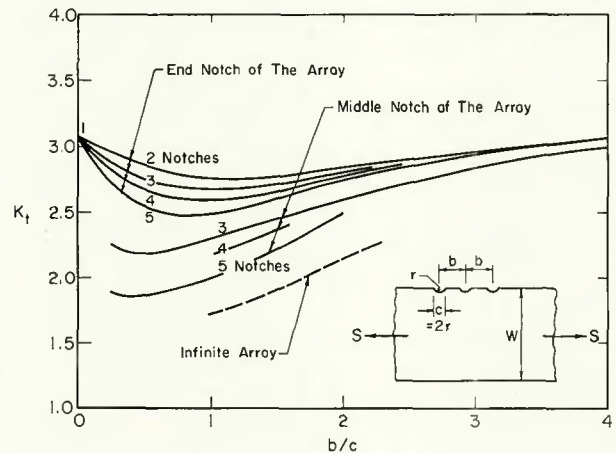


Fig. 12—Elastic stress concentration factor for periodic arrays of semicircular surface notches⁵

Table 2—Comparison of Calculated and Measured Fatigue Stress Concentration Factor, $K_t^{(a)}$

| Material | a (in.) | Calculated K_t | | Measured K_t |
|-------------------|---------|------------------|------------|----------------|
| | | Semicircular | Elliptical | |
| A572 | 0.010 | 1.30 | 1.83 | 1.28 |
| A514 | 0.0053 | 1.48 | 2.16 | 1.48 |
| A514 (normalized) | 0.012 | 1.24 | 1.80 | 1.53 |

^(a) K_t values are for roughest specimens tested (0.011 in. RMS) compared to smoothest specimens tested (0.001 in. RMS).

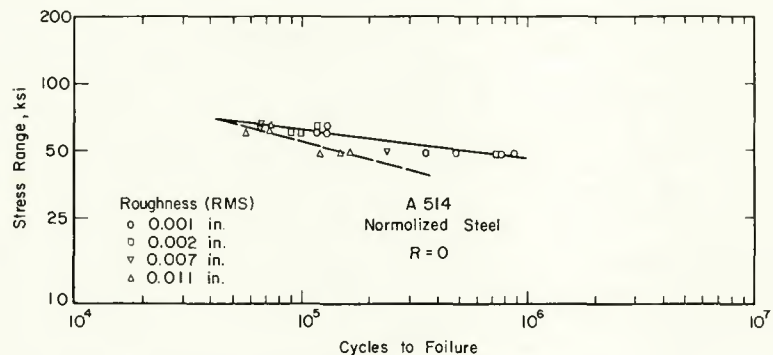


Fig. 13—S-N diagram for normalized A514 steel specimens

smoothest oxygen cut specimen results were taken for the numerator and the roughest specimen results for the denominator. The values of stress were

the stresses which caused failure in 10^6 cycles. These stresses were taken from the curves of Figs. 6 and 7. The close agreement in Table 2 between mea-

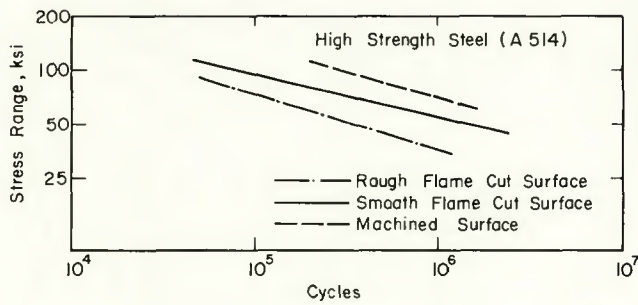


Fig. 14—Comparison of machined and oxygen-cut surface fatigue resistance—A514 steel specimens

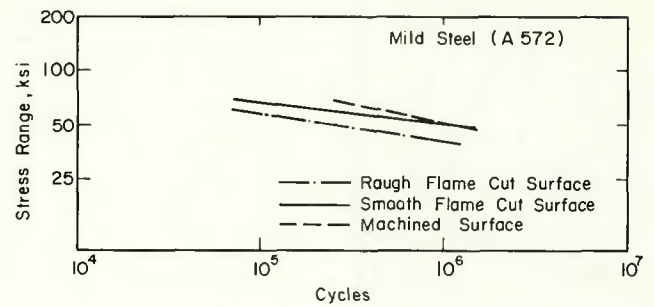


Fig. 15—Comparison of machined and oxygen-cut surface fatigue resistance—A572 steel specimens

sured values of K_f and those calculated for an array of semicircular notches indicates that the model is valid and that the approximations are reasonable; however, further data would be useful.

Accordingly, specimens of the A514 steel were normalized after oxygen cutting and tested subsequent to wire brushing to remove the scale from the normalizing treatments. Hardness profiles demonstrated that aside from some decarburization at the surface the hardness was uniform. The tensile properties are shown in Table 1. Fatigue results are shown in Fig. 13 and experimental and calculated K_f values are compared in Table 2. Although the agreement is not as good as for the as-cut surfaces, it is qualitatively correct.

A further refinement of the model would be to take into account the layer of altered microstructure at the surface of the flame cut specimens. Here the hardness and S_u would be higher, and the (a) value lower. This would have the effect of increasing the calculated K_f values. It is felt that such refinements are unjustified in the present work, considering the approximations which have been used. The situation is further complicated by the changes in geometry as the fatigue crack propagates, by residual stresses and by simultaneous changes in microstructure below the surface.

Comparison of Oxygen Cut and Machined Surfaces

The ultimate objective of oxygen cutting is to achieve an economy in fabrication; however, this must be done without unwarranted degradation in properties. In order to evaluate the quality of the trade-off between economy and performance, comparisons were made between oxygen cut and machined specimens for the same specimen geometry and nominal stress

levels. A rough indication could be obtained by noting that three of the lateral surfaces of the fatigue specimens were machined and one was in the oxygen cut condition, yet nearly all fatigue cracks initiated at the oxygen cut surface. Further verification of the superiority of the machined surface was obtained by performing a limited number of fatigue tests on fully machined specimens of the same geometry, base metal and stress level.

Figures 14 and 15 show the results for the machined specimens in comparison with the lives for the smoothest and roughest oxygen cut specimens. From the limited amount of data it is impossible to draw unequivocal conclusions, yet it is clear that at high stress levels, machined surfaces are superior to even the smoothest oxygen cut surface. At a lower stress level, it appears that a well-made oxygen cut surface may result in no degradation of fatigue life.

Extrapolation to lower stresses in Figs. 14 and 15 indicates that machined surfaces may in fact be inferior to a smooth oxygen cut. This may be a case of the benefits of residual stress and microstructural alteration as a result of oxygen cutting more than compensating for the geometrical effects of a rough surface, resulting in an overall improvement in fatigue life.

Conclusions

1. The fatigue resistance of the smoothest oxygen cut surface is greatest for the high strength steel A514. However, at lives equal to or greater than 10^6 cycles, the difference between A514 and the A572 results diminishes such that the two steels give approximately the same fatigue strength.

2. Increasing surface roughness has the greatest effect on stress level in the

A514 steel and only a moderate effect on the A572 steel.

3. Oxygen cut surfaces of both steels have fatigue resistances inferior to machined surfaces in the life range 10^4 to 10^6 cycles. Extrapolation of the test results to longer lives would indicate the possibility that smooth oxygen cut surfaces may out-perform fully machined surfaces at lives greater than 10^6 cycles.

4. The influence of surface roughness on fatigue life can be qualitatively understood by considering the surface roughness to be a periodic array of surface notches.

Acknowledgments

This work was sponsored by the Caterpillar Tractor Company, Peoria, Illinois. The suggestions and cooperation of Mr. Willis Fildes and Mr. Cal Loyd of that company were important contributions to this work. The use of the testing facilities of the Civil Engineering Department of the University of Illinois are also appreciated.

References

1. Koenigsberger, F., and Garcia-Martin, Z., "Fatigue Strength of Flame-Cut Specimens in Bright Mild Steel," *British Welding Journal*, January 1955, pp. 37-41.
2. Koenigsberger, F., and Green, H. W., "Fatigue Strength of Flame-Cut Specimens in Black Mild Steel," *British Welding Journal*, July 1955, pp. 313-321.
3. "The Properties of Flame-Cut Edges," Netherlands Institute of Welding, Final Report of Working Group 1913, May 1973.
4. Goldberg, F., "Influence of Thermal Cutting and Its Quality on the Fatigue Strength of Steel," *Welding Journal*, 52(9), Sept. 1973, Res. Supp., pp. 392-s to 404-s.
5. Peterson, R. E., *Stress Concentration Factors*, Wiley and Sons, Inc., New York, 1974.
6. Peterson, R. E., "Notch Sensitivity," *Metal Fatigue*, Chapter 13, Sines and Waisman, Editors, McGraw-Hill Book Co., Inc., 1959.

AUTHORS . . . See page 244-s.